A DNA repair-independent role for alkyladenine DNA glycosylase in alkylation-induced unfolded protein response

Larissa Milano[a,b,c,d], Clara F. Charlier[a], Rafaela Andreguetti[a], Thomas Cox[a], Eleanor Healing[e], Marcos P. Thomé[f], Ruan M. Elliott[e], Leona D. Samson[g,h], Jean-Yves Masson[c,d], Guido Lenz[b,f], João Antonio P. Henriques[b,f], Axel Nohturfft[i], and Lisiane B. Meira[a,1]

[a]Department of Clinical and Experimental Medicine, Faculty of Health and Medical Sciences, University of Surrey, GU2 7WG Guildford, United Kingdom; [b]Center of Biotechnology, Federal University of Rio Grande do Sul, 91501-970 Porto Alegre, Brazil; [c]Genome Stability Laboratory, CHU de Quebec Research Center, HDQ Pavilion, Oncology Axis, Québec City, QC G1R 3S3, Canada; [d]Department of Molecular Biology, Medical Biochemistry and Pathology, Laval University Cancer Center, Quebec City, QC G1V 0A6, Canada; [e]Department of Nutritional Sciences, Faculty of Health and Medical Sciences, University of Surrey, GU2 7XH Guildford, United Kingdom; [f]Department of Biophysics, Federal University of Rio Grande do Sul, 91501-970 Porto Alegre, Brazil; [g]Department of Biological Engineering, Massachusetts Institute of Technology, Cambridge, MA 02139; [h]Department of Biology, Massachusetts Institute of Technology, Cambridge, MA 02139; and [i]Molecular and Clinical Sciences Research Institute, St. George's University of London, SW17 0RE London, United Kingdom

Edited by Susan Wallace, Microbiology & Molecular Genetics, University of Vermont Medical Center, Burlington, VT; received June 25, 2021; accepted January 8, 2022 by Editorial Board Member James E. Cleaver

Alkylating agents damage DNA and proteins and are widely used in cancer chemotherapy. While cellular responses to alkylation-induced DNA damage have been explored, knowledge of how alkylation affects global cellular stress responses is sparse. Here, we examined the effects of the alkylating agent methylmethane sulfonate (MMS) on gene expression in mouse liver, using mice deficient in alkyladenine DNA glycosylase (Aag), the enzyme that initiates the repair of alkylated DNA bases. MMS induced a robust transcriptional response in wild-type liver that included markers of the endoplasmic reticulum (ER) stress/unfolded protein response (UPR) known to be controlled by XBP1, a key UPR effector. Importantly, this response is significantly reduced in the *Aag* knockout. To investigate how AAG affects alkylation-induced UPR, the expression of UPR markers after MMS treatment was interrogated in human glioblastoma cells expressing different AAG levels. Alkylation induced the UPR in cells expressing AAG; conversely, *AAG* knockdown compromised UPR induction and led to a defect in XBP1 activation. To verify the requirements for the DNA repair activity of AAG in this response, *AAG* knockdown cells were complemented with wild-type *Aag* or with an *Aag* variant producing a glycosylase-deficient AAG protein. As expected, the glycosylase-defective Aag does not fully protect *AAG* knockdown cells against MMS-induced cytotoxicity. Remarkably, however, alkylation-induced XBP1 activation is fully complemented by the catalytically inactive AAG enzyme. This work establishes that, besides its enzymatic activity, AAG has noncanonical functions in alkylation-induced UPR that contribute to cellular responses to alkylation.

alkylating agents | unfolded protein response | DNA damage | ER stress | base excision repair

Organisms are constantly exposed to a variety of stresses that can result in macromolecular injury and cellular dysfunction (1, 2). Reactive compounds that originate from the environment or arise from intracellular processes can damage nucleic acids, proteins, and lipids. Exposure to stress triggers highly conserved signaling pathways, such as the DNA damage response (DDR) and endoplasmic reticulum (ER) stress responses that act to restore homeostasis. Failure of cells and tissues to properly respond to stress and damage underpins the pathogenesis of many diseases (2, 3).

Alkylating agents represent an abundant and ubiquitous family of reactive chemicals that can damage DNA, RNA, and proteins (4). Sources of alkylating agents include by-products of metabolism (5) and environmental nitroso-compounds such as nitrosamines that are present in pollutants and food preservatives and that have recently been found in common medications (6–8). Exposure to alkylating agents has been associated with cancer, type 2 diabetes, nonalcoholic steatohepatitis, and neurodegenerative diseases (9, 10). On the other hand, because they effectively kill dividing tumor cells, alkylating agents are commonly employed as cancer chemotherapeutic agents.

Alkylation-induced DNA base lesions are primarily repaired by the base excision repair (BER) pathway, initiated by the enzyme alkyladenine DNA glycosylase (AAG, also known as N-methylpurine DNA glycosylase or MPG) (5). AAG excises damaged bases from the DNA phosphodiester backbone, generating an abasic site. Subsequently, an apurinic/apyrimidinic endonuclease cleaves the phosphodiester backbone at the abasic site, creating a single-strand break (SSB) that contains 3′OH and 5′deoxyribose-5-phosphate (5′dRP) termini. Accurate repair of SSBs that are generated during BER requires

Significance

Stress response pathways, such as the DNA damage response and the UPR, are critical in the etiology and treatment of cancer and other chronic diseases. Knowledge of an interplay between ER stress and genome damage repair is emerging, but evidence linking defective DNA repair and impaired ER stress response is lacking. Here, we show that AAG is necessary for UPR activation in response to alkylating agents. AAG-deficient mice and human cancer cells are impaired in alkylation-induced UPR. Strikingly, this defect can be complemented by an AAG variant defective in glycosylase activity. Our studies suggest that AAG has noncanonical functions and identify AAG as a point of convergence for stress response pathways. This knowledge could be explored to improve cancer treatment.

Author contributions: L.M., L.D.S., A.N., and L.B.M. designed research; L.M., C.F.C., R.A., T.C., E.H., M.P.T., R.M.E., A.N., and L.B.M. performed research; L.D.S., J.-Y.M., G.L., and J.A.P.H. contributed new reagents/analytic tools; L.M., R.M.E., G.L., A.N., and L.B.M. analyzed data; and L.M., A.N., and L.B.M. wrote the paper.

The authors declare no competing interest.

This article is a PNAS Direct Submission. S.W. is a guest editor invited by the Editorial Board.

[1]To whom correspondence may be addressed. Email: l.meira@surrey.ac.uk.

This article contains supporting information online at http://www.pnas.org/lookup/suppl/doi:10.1073/pnas.2111404119/-/DCSupplemental.

Published February 23, 2022.

PARP (poly(ADP ribose) polymerase) (5). PARP binds to SSBs and is activated, leading to the synthesis of poly(ADP ribose) chains and the recruitment of the scaffolding protein XRCC1, DNA polymerase β, and ligase to the SSB. DNA polymerase β removes the 5′dRP and carries out single-nucleotide gap filling synthesis. The nicked DNA is then ligated by DNA ligase I or the XRCC1/Ligase III complex (5, 11). The flux of intermediates through this pathway must be efficiently coordinated because BER intermediates, such as abasic sites and SSB, are toxic (12–14). It has been shown that BER flux imbalance due to AAG overexpression exacerbates alkylation toxicity (15, 16). Moreover, elevated AAG expression has been associated with poor prognosis in patients with glioblastoma, an aggressive type of brain cancer often treated with alkylating agents (17, 18).

While the effects of alkylation on DNA have been well studied, cellular responses to alkylation-induced protein damage are still poorly understood. Alkylation treatment of yeast and mammalian cells induces hallmarks of ER stress, involving the UPR (19–21). The UPR is an adaptive signal transduction pathway orchestrated by the ER that is important for the maintenance of a functional proteome. A wide range of perturbations can result in ER stress, such as accumulation of unfolded/misfolded proteins, disturbances in calcium homeostasis, hypoxia, oxidative stress, and viral infections (22). The following three ER-resident transmembrane proteins initiate the UPR: inositol-requiring kinase 1 (IRE1), activating transcription factor 6 (ATF6), and protein kinase-like ER kinase (PERK). These transducers are negatively regulated by chaperones that dissociate during ER stress, leading to activation of the UPR (22). The UPR usually acts as a cytoprotective mechanism, but chronic ER stress leads to cell death (22). UPR activation was shown to play a key role in cancer by enabling tumor cells to tolerate and thrive in a hostile environment of nutrient deprivation, hypoxia, and low pH, which in turn contributes to cellular transformation, tumor growth, metastasis, and resistance to chemo/radiotherapy (23).

AAG was shown to be the major DNA glycosylase activity for the excision of alkylated lesions in mouse liver (24). To better characterize the outcomes of alkylation damage, we analyzed gene expression in livers of wild-type and Aag-deficient mice that had been exposed to the model alkylating agent methylmethane sulfonate (MMS). Our findings show that alkylation treatment induces ER stress and the UPR in vivo. Surprisingly, alkylation-induced expression of ER stress genes was significantly reduced in $Aag^{-/-}$ livers. To probe the mechanism underlying this relationship, we employed a panel of human glioblastoma cell lines expressing different levels of AAG and DNA repair-proficient and -deficient mouse AAG variants. As in mouse liver, we find AAG is required for optimal UPR induction after alkylation treatment in human glioblastoma cells. Moreover, we show that a repair-defective AAG variant unable to complement alkylation-induced PARP activation and survival is proficient in the activation of the bZIP transcription factor X-box binding protein 1 (XBP1), a key regulator of the UPR. This striking result indicates AAG has noncanonical roles in alkylation-induced UPR induction. Finally, considering the dual survival or cell death outcome of the UPR, we also examined the effect of AAG status on cellular sensitivity to alkylating agents alone or combined with a pharmacological activator of ER stress.

Results

Aag Is Required for Alkylation-Induced ER Stress Response Mediated by Xbp1 Activation. Alkylating agents activate both the DDR and the UPR. To explore potential connections between these pathways, we compared alkylation-induced changes in livers of wild-type and Aag-deficient mice. Wild-type and $Aag^{-/-}$ animals, in triplicate, were injected with a mild, nonlethal dose of the direct acting alkylating agent MMS, and liver tissue was harvested after 6 h. This MMS dose and time point have been previously characterized, and for both genotypes, no difference in liver histology or weights between controls or MMS-treated cohorts was noted by pathological examination (16).

Following RNA extraction, transcriptome analysis was performed using gene chip arrays. The scale and distribution of the data on the 12 arrays were comparable (*SI Appendix*, Fig. S1*A*). Changes in expression associated with a fold change of at least 1.75 (false discovery rate-adjusted $P \leq 0.05$) were considered as significant, and the affected genes were marked for further analysis. Only minor differences in gene expression were observed under control conditions between wild-type and Aag-deficient liver, indicating that the absence of Aag does not cause significant stress under basal metabolic conditions (Fig. 1*A*, *SI Appendix*, Fig. S1*B*).

MMS treatment led to substantial differences in gene expression between wild-type and $Aag^{-/-}$ mice, with 4.7-fold more genes differentially expressed in wild-type, and with minimal overlap (Fig. 1*B*). This indicates that the absence of Aag affects alkylation-induced gene expression after MMS treatment.

We next performed gene set enrichment analyses using libraries provided by the Enrichr database (25, 26). As expected from studies with cultured cells (19–21, 27), genes induced by MMS in wild-type liver are enriched for gene sets related to ER stress (Gene Ontology [GO]:0034976, positive false discovery rate [p-FDR] = 8.7E-06) and the UPR (GO:0030968, p-FDR = 3.2E-05), and we saw overlaps with multiple gene sets induced by drugs that are known to cause ER stress (Dataset 2 and *SI Appendix*, Fig. S2). However, of the 12 ER stress response genes induced in wild-type, only 2 are also induced in the $Aag^{-/-}$ liver (Dataset 2). Importantly, genes induced in an Aag-dependent manner significantly overlap with genes in the transcriptional network activated by XBP1 (Fig.1 *C* and *D*), a transcription factor which promotes the expression of several ER stress-related genes (22). These networks include 1) genes upregulated in cells expressing a constitutively active form of Xbp1 (p-FDR = 3E-13; Dataset 2) (28), 2) physical Xbp1 targets according to mouse liver chromatin immunoprecipitation sequencing (ChIP-seq) data (p-FDR = 1.6E-14) (29), and 3) the Xbp1 transcriptional correlation network (p-FDR = 2.5E-10) (30).

Further supporting a potential role for Xbp1 in alkylation-induced gene expression, genes that are downregulated following MMS treatment are enriched for independent sets of genes suppressed in cells overexpressing constitutively active Xbp1 (p-FDR = 4.1E-09 to 9.3E-05; Dataset 2) (28, 31). No such enrichments are seen for genes affected by Aag deficiency alone, and Fig. 1*E* shows that XBP1 targets are more highly induced in wild-type livers than in $Aag^{-/-}$ livers. These data indicate that MMS induces the expression of Xbp1 targets in an Aag-dependent manner.

Generation of transcriptionally active XBP1 protein requires unconventional splicing of its mRNA, a process initiated by the ER stress-induced endonuclease IRE1α (32). We asked, therefore, whether AAG might be required for maximal XBP1 splicing in response to MMS. Experiments were carried out with T98G cells, which are derived from glioblastoma, a type of cancer frequently treated with alkylating chemotherapy agents (33). MMS induced XBP1 splicing in wild-type T98G cells; however, when AAG expression and activity were reduced by RNA interference (RNAi) (*SI Appendix*, Fig. S3 *A–C*), XBP1 splicing was substantially diminished (Fig. 1 *F* and *G*). Of note, AAG depletion did not affect cellular viability of T98G cells in the absence of treatment. Cells transfected with a nonsilencing control short hairpin RNA (shRNA; shNS) displayed some XBP1 splicing even in the absence of MMS, which may be due

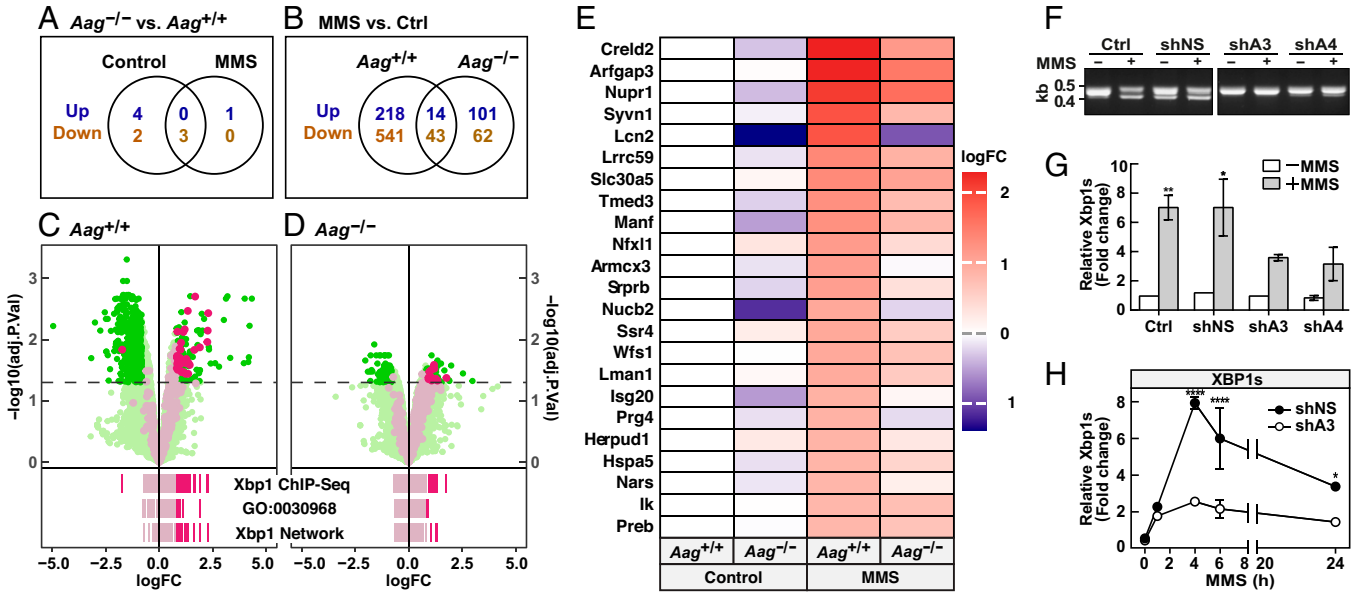

Fig. 1. Aag modifies the transcriptional response to alkylation and is required for XBP1 splicing induced by alkylation. Wild-type and Aag-deficient mice ($n = 3$) were injected with MMS or solvent and euthanized 6 h later. Liver RNA was analyzed using oligonucleotide microarrays. (*A* and *B*) Venn diagrams indicate the number of differentially regulated probe sets ($\log_2$ fold change [FC] of ≥1.75; FDR-adjusted $P \leq 0.05$). Detailed gene expression data are given in Dataset 1. (*C* and *D*) Negative $\log_{10}$ adjusted *P* values (adj.P.Vals) are plotted against $\log_2$ (FC). Dashed line, negative $\log_{10}$ (0.05). Xbp1 targets according to mouse liver ChIP-seq data (29) are highlighted in gray or in magenta where $|\log_2$ (FC)| is ≥1.75 and p-FDR is ≤0.05. Rug plots below indicate the $\log_2$ (FC) of genes annotated as Xbp1 targets (Xbp1 ChpSq), ER stress response (GO:0030968), or Xbp1 transcriptional correlation network (Xbp1 Netwrk); where $|\log_2$ (FC)| of <1.75 genes are marked in gray; lines are drawn at 60% transparency. (*E*) Heatmap indicating $\log_2$ FCs of known Xbp1 target genes (28) induced by MMS in wild-type liver. (*F*) Cells were treated with 2.5 mM MMS, and 6 h later XBP1 splicing was analyzed by RT-PCR and agarose gel electrophoresis. (*G*) Quantification of XBP1 splicing by RT-qPCR 6 h after treatment with MMS (2.5 mM) $*P < 0.05$, $**P < 0.01$. (*H*) Quantification of XBP1 splicing after treatment with MMS for the indicated time. $*P < 0.05$, $****P < 0.0001$.

to stress caused by the cytomegalovirus (CMV)-driven knockdown system we employed (Fig. 1*F*; *SI Appendix*, Fig. S4). A time curve of MMS treatment showed that XBP1 splicing peaked after 4 h, and splicing was reduced in AAG-deficient cells at all time points up to 24 h (Fig. 1*H*).

We also compared XBP1 splicing in A172 glioblastoma cells that express low endogenous levels of AAG, versus A172 cells stably expressing a green fluorescent protein (GFP)-AAG fusion protein (*SI Appendix*, Fig. S3). Differential AAG expression and activity in these cells were verified by qPCR, immunoblotting, and enzyme assay (*SI Appendix*, Fig. S3 *D–F*). XBP1 splicing could not be detected in parental A172 cells (Ctrl) or in A172 cells expressing just GFP, while splicing was effective in cells expressing GFP-AAG, albeit in a manner that is apparently independent of MMS treatment (*SI Appendix*, Fig. S4). The XBP1 splicing observed in the absence of MMS treatment is likely due to the CMV-driven GFP expression by the expression vector we employed for these experiments. Nevertheless, when *XBP1* mRNA was analyzed by qPCR, MMS-induced splicing was detectable in parental A172 and in GFP cells, and splicing increased about twofold in cells over expressing GFP-AAG (*SI Appendix*, Fig. S4).

AAG Modulates Expression of XBP1 Target Genes in Glioblastoma Cells after Alkylation Treatment. To verify the effects of AAG on XBP1 activation, we measured the mRNA levels of *HSPA5* (BiP/GRP78) and *HERPUD1*, two prominent markers of ER stress and known targets of XBP1 (28, 29). In T98G shNS, which expresses abundant levels of AAG (*SI Appendix*, Fig. S3), MMS treatment increases *BiP* and *HERPUD1* mRNA threefold to fourfold ($P < 0.05$; $P < 0.01$), with BiP peaking after 6 h, while HERPUD1 continued to increase for up to 24 h; in *AAG* knockdown cells, by contrast, *BiP* is not induced by MMS, and *HERPUD1* induction is significantly reduced (Fig. 2*A*). Immunoblotting confirmed that MMS-induced BiP expression is lower in *AAG* knockdown cells (Fig. 2*B*), reaching a maximum at 6 h (*SI Appendix*, Fig. S5 *A* and *B*). Regulation of BiP by MMS was also studied in GFP-transfected A172 cells, which express low levels of endogenous AAG versus cells overexpressing an AAG-GFP fusion protein. Once again, AAG expression positively correlated with MMS-dependent *BiP* induction; *BiP* mRNA levels were higher in *AAG* overexpressing cells than in control cells after MMS treatment at all time points tested (*SI Appendix*, Fig. S5*C*). Western blotting confirmed that MMS treatment induced BiP to higher levels in the AAG overexpressing A172 cells (Fig. 2*C*). These data further support the conclusion that MMS triggers an ER stress response through a pathway involving AAG and XBP1.

The Role of AAG Is Specific for Alkylation-Induced ER Stress. To gauge whether AAG might be important for other branches of the UPR, we analyzed the mRNA levels of ATF4 and DDIT3/CHOP, which are controlled through the PERK and ATF6 pathways (34). Both ATF4 and CHOP were induced by MMS in control T98G cells, but only ATF4 induction was reduced in AAG-depleted cells (Fig. 2*A*).

Next, we asked whether the role of AAG in the UPR is specific to alkylation damage. To address this question, we analyzed the effects of the well-studied ER stressor thapsigargin, which depletes ER Ca^{2+} by blocking SarcoEndoplasmic Reticulum Calcium (SERCA) ATPases (35). Experiments with T98G and A172 glioblastoma lines expressing varying levels of AAG showed that thapsigargin induced splicing of XBP1 (*SI Appendix*, Fig. S6*A*); induced the transcription of BiP, HERPUD1, ATF4, or CHOP (*SI Appendix*, Fig. S6 *B–F*); and increased BiP protein expression (*SI Appendix*, Fig. S6*G*) in an AAG-independent manner. These results are consistent with

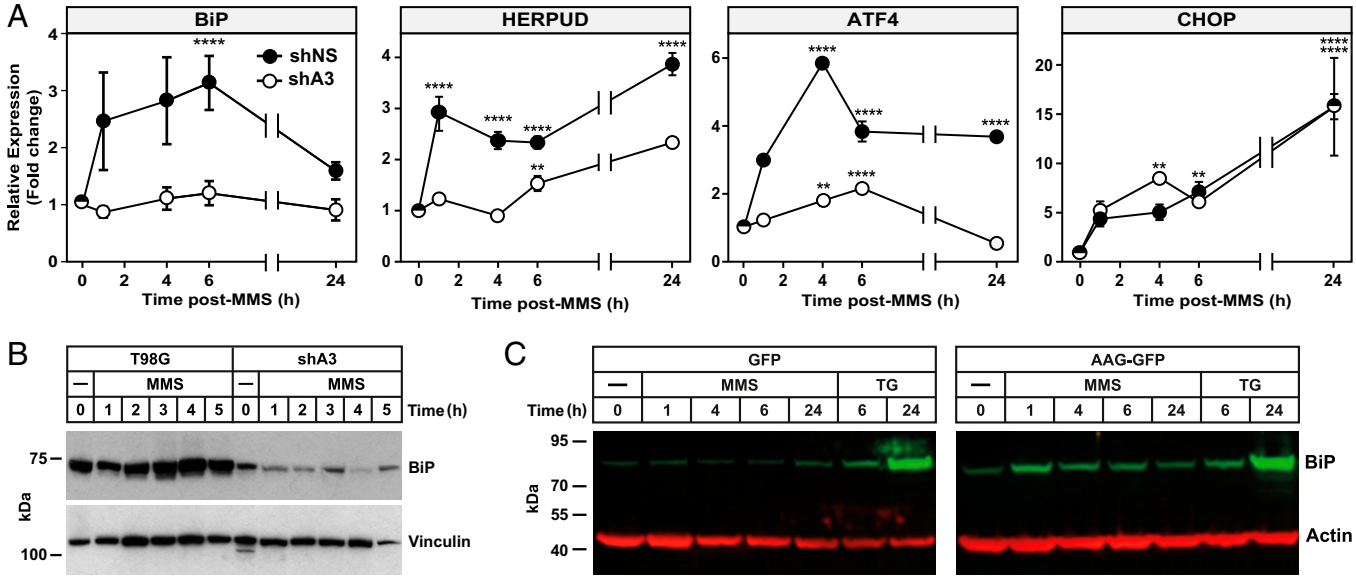

Fig. 2. AAG modulates the expression of XBP1 target genes in glioblastoma cells after alkylation treatment. Cells were treated with 2.5 mM MMS or 300 nM thapsigargin (TG), as indicated. (*A*) Quantification of *BiP*, *HERPUD*, *ATF4*, and *CHOP* mRNA levels by qPCR. (*B*) BiP protein levels in shNS and shA3 cells. (*C*) BiP protein levels were detected by immunoblotting. The results are expressed as mean values ± SEM from three independent experiments $^{**}P < 0.01$, $^{****}P < 0.0001$.

the model that AAG affects specifically alkylation-induced ER stress through a pathway that feeds into the XBP1 and likely the PERK branches of the UPR.

Evidence for a Noncanonical AAG Role in Alkylation-Induced UPR Induction. Alkylation DNA damage can affect gene expression by direct structural hindrance of the transcriptional machinery or due to activation of the DNA repair pathway. We therefore assessed whether the DNA repair activity of AAG is required to activate stress responses. We transfected *AAG* knockdown shA3 cells with an empty vector (shA3-EV cells), or with plasmids expressing either wild-type mouse Aag (shA3-WT cells) or an enzymatically deficient Y147I/H156L double mutant (shA3-MUT cells). The Y147I/H156L mutant is the mouse equivalent of the characterized human Y127I/H136L mutant, which is catalytically inactive despite retaining some ability to bind damaged DNA (36). Expression of transfected mouse Aag in the human knockdown cells was possible due to species-specific mismatches in the sequence targeted by the shA3 shRNA, and mouse Aag expression was confirmed by Western blotting (Fig. 3*A*).

Using these cell lines, we first compared the ability of wild-type and mutant mouse Aag to protect cells from alkylation-induced cytotoxicity. At the highest MMS concentration, AAG-deficient shA3-EV cells were more sensitive than parental T98G cells, and expression of Aag-Y147I/H156L failed to rescue survival relative to that of cells expressing wild-type Aag (Fig. 3*B*). To confirm the complementation of glycosylase activity, we employed a fluorescently labeled oligonucleotide complex containing a single hypoxanthine as the Aag substrate (labeled "substrate," *SI Appendix*, Fig. S7). Excision of the hypoxanthine base by recombinant AAG following alkali cleavage by NaOH generates a product of the expected size (labeled "product"). Using this assay, we can detect a time and nuclear extract concentration-dependent decrease in glycosylase activity in *AAG* knockdown cells compared to control (Fig. 3*C*), and this defect is complemented when cells are transfected with wild-type Aag, but not with the Aag-Y147I/H156L double mutant (Fig. 3 *D* and *E*).

AAG-initiated BER leads to the generation of repair intermediates that activate PARP (12). PARP is activated at SSBs to synthesize a polymer of ADP ribose (PAR) attached to itself plus other acceptor proteins usually associated with DNA transactions and shaping cellular outcome to a variety of stress conditions (16). Thus, we next assessed total cellular PARylation in these cell lines. Western blot analyses against PAR using total cell lysates prepared in the presence of a PARG inhibitor showed that MMS treatment increased total cellular PAR levels in the control cells T98G and shNS and in the knockdown cells expressing wild-type Aag, but not in knockdown cells alone or expressing the Aag-Y147I/H156L double mutant (*SI Appendix*, Fig. S8). Because the addition of a PARG inhibitor may also promote PAR accumulation that is unrelated to MMS treatment, we also performed these experiments in the absence of the PARG inhibitor (Fig. 3 *F* and *G*). Under these conditions, we show that PAR is undetectable in nonstressed cells and that PAR formation peaks at 15-min post-MMS treatment, decreasing to background levels 60 min post-treatment. Once again, PAR levels are increased in control cells and in the knockdown cells expressing wild-type Aag, but not in knockdown cells alone or expressing the Aag-Y147I/H156L double mutant (Fig. 3 *F* and *G*).

Phosphorylation of the histone variant H2AX is a key event in the DDR following alkylation damage. We previously showed AAG-initiated BER is necessary for alkylation-induced γH2AX activation (12). Indeed, we confirm that *AAG* knockdown cells show reduced γH2AX foci formation after MMS treatment (Fig. 3 *G* and *H*). Surprisingly, however, we observe significantly increased levels of γH2AX foci in *AAG* knockdown cells complemented with either wild-type Aag or the Aag-Y147I/H156L double mutant, albeit at reduced levels in the mutant-complemented cells (Fig. 3 *G* and *H*). Together, these results suggest that despite a repair defect as shown by reduced glycosylase activity, reduced survival to alkylation, and defective alkylation-induced PARylation, the mutated Aag-Y147I/H156L protein retains some ability to induce γH2AX.

Finally, we tested whether the Aag-Y147I/H156L double mutant could restore the splicing of XBP1 and expression of other markers of UPR (Fig. 4). Mutant and wild-type mouse Aag expression restores XBP1 splicing and, at least partially, other markers of ER stress (Fig. 4 *A*–*D*). In *AAG* knockdown cells complemented with wild-type Aag, MMS treatment significantly induces BiP, HERPUD, and XBP1s, while in *AAG* knockdown cells complemented with the Aag-Y147I/H156L double

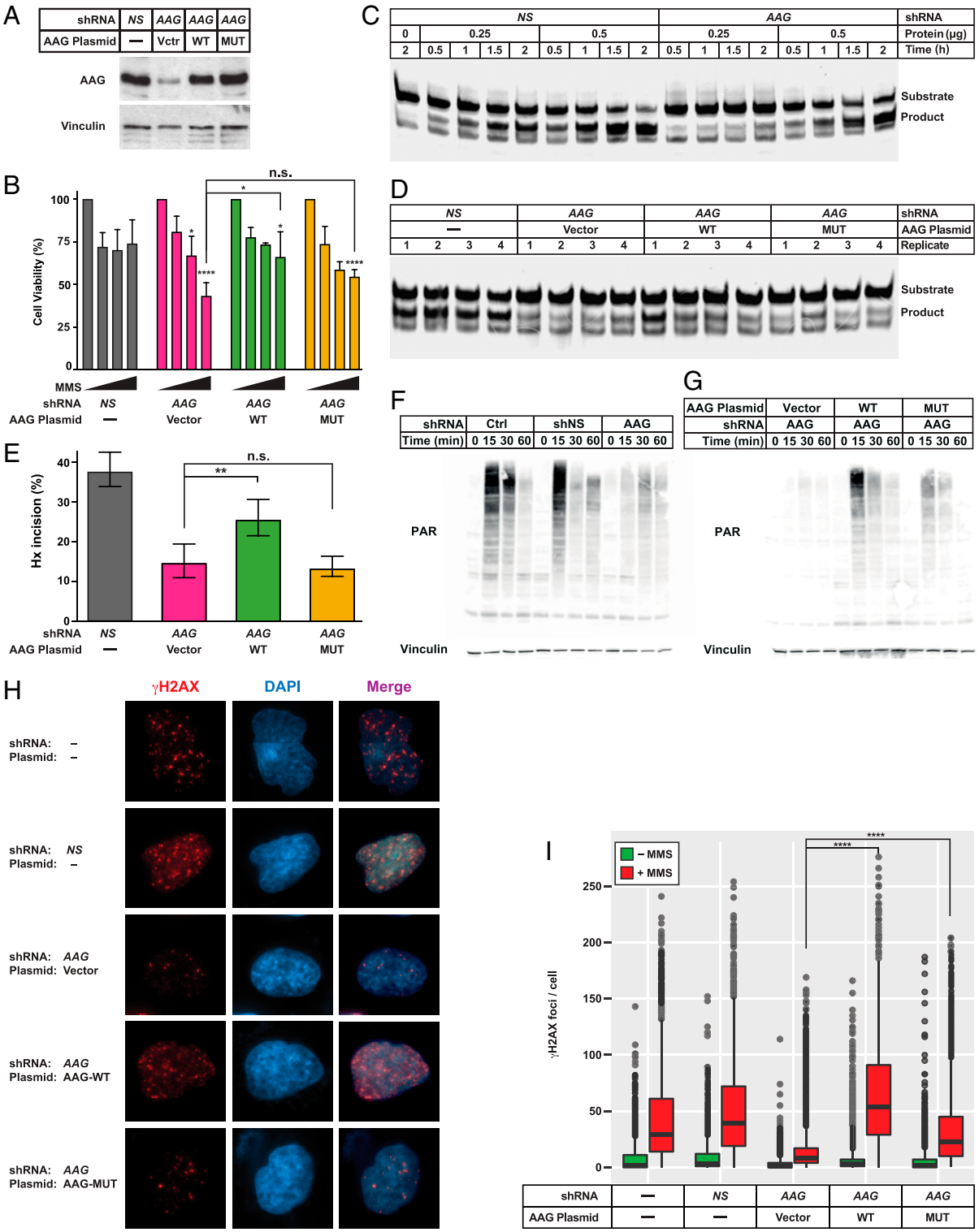

Fig. 3. The mAag Y147I, H156L double-mutant variant is defective in glycosylase activity and alkylation-induced PARylation but retains the ability to induce γH2AX foci after MMS treatment. (*A*) Western blot of *AAG* knockdown shA3 cells stably transfected with plasmids; empty vector (Vctr), expressing wild-type (WT) and Y147I, H156L double-mutant (MUT) mouse Aag. (*B*) Cell viability of control and complemented shA3 cells exposed to MMS (0, 60, 120, and 250 μM) for 1 h followed by 24-h incubation in drug-free media. Data were analyzed by two-way ANOVA with Dunnett's multiple comparisons test. n.s., not significant. (*C*) AAG activity was assessed by incubation of 0.25 or 0.5 μg of nuclear extract with a fluorescently labeled hypoxanthine containing oligonucleotide substrate for increasing times at 37 °C. Reaction products were run on a 15% denaturing polyacrylamide gel and visualized by fluorescence imaging. (*D*) AAG activity in different genotypes was assessed as in *C* (0.25 μg protein, 1.5 h at 37 °C, $n = 4$ independent lysates). (*E*) Fluorometric quantification of *D* (product band divided by total). Means were compared by one-way ANOVA. (*F* and *G*) Control (Ctrl) and shA3 cells (*F*) and shA3 cells complemented with wild-type or Y147I/H156L double-mutant mouse Aag (*G*) were treated with MMS in the absence of PARG inhibitor and harvested 0, 15, 30, or 60 min after the addition of MMS. Total PAR levels were examined by Western blotting against PAR. (*H* and *I*) Representative immunofluorescence images (*H*) and quantification (*I*) of γH2AX foci in control and complemented shA3 cells exposed to MMS for 1 h followed by 1 h in drug-free media ($n = 3$; one-way ANOVA). $^*P < 0.05$, $^{**}P < 0.01$, $^{****}P < 0.0001$.

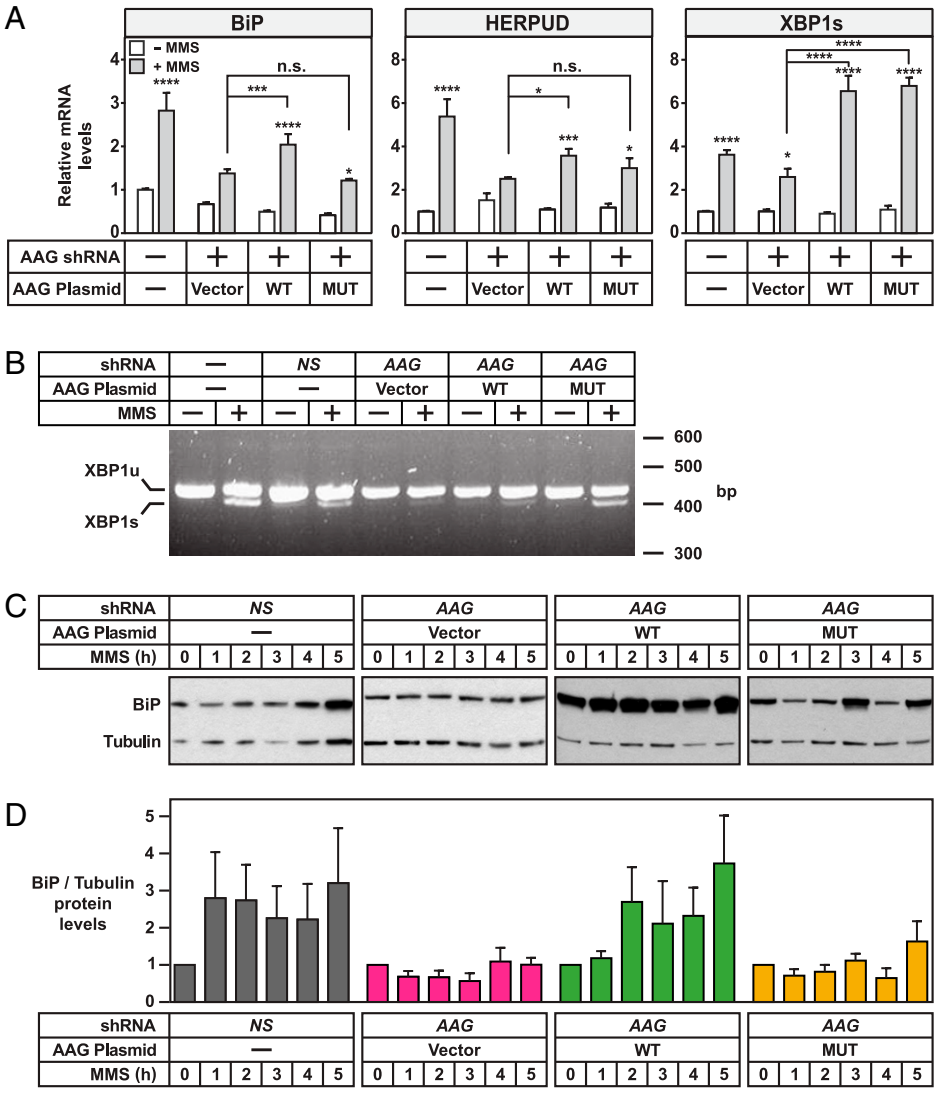

Fig. 4. AAG glycosylase activity is not required for alkylation-induced XBP1 splicing. (*A*) Quantification of *BiP*, *HERPUD*, and spliced *XBP1* mRNA levels by qPCR in cells treated with 2.5 mM MMS for 1 h followed by 5-h incubation in drug-free media ($n = 3$, two-way ANOVA with Dunnett's multiple comparisons test). (*B*) RT-PCR analysis shows XBP1 splicing in T98G, shNS, and *AAG* knockdown cells complemented with wild-type or Y147I/H156L double mutant mouse Aag treated with 0.5 mM MMS for 1 h followed by 1 h in drug-free media. (*C*) Temporal characterization of BiP protein levels in control and complemented *AAG* knockdown cells after treatment with 2.5 mM MMS (*D*) Quantification of BiP protein levels determined by Western blotting in three independent experiments. BiP results were normalized to α-tubulin and are expressed relative to untreated control (mean ± SEM). $*P < 0.05$, $***P < 0.001$, $****P < 0.0001$.

mutant, significant induction after MMS treatment is seen solely for XBP1s (Fig. 4*A*). Strikingly, when analyzed by agarose gel electrophoresis, *AAG* knockdown cells expressing the Aag-Y147I/H156L double mutant display more prominent XBP1 splicing than cells complemented with wild-type Aag (Fig. 4*B*). In addition, to verify that these findings are not limited to mouse Aag, we show that the XBP1 splicing defect in the *AAG* knockdown cells can be fully rescued by transient transfection with knockdown-resistant wild-type and glycosylase-deficient Y127I/H136L double mutant human AAG complementary DNAs (cDNAs) (*SI Appendix*, Fig. S9). Taken together, these results strongly suggest that AAG can mediate alkylation-induced XBP1 splicing independently of its glycosylase activity and in a PARP-independent manner. Indeed, we find that alkylation-induced XBP1 splicing is unaffected in *PARP* knockout cells (39) (*SI Appendix*, Fig. S10). We thus propose that AAG has a noncanonical role outside the BER pathway in mediating ER stress induction in response to alkylation.

AAG-Mediated UPR Induction Plays a Role in Survival to Alkylation. Activation of the UPR has been proposed as a mechanism underpinning the glioblastoma response to treatment. UPR downregulation increases glioblastoma sensitivity to gamma radiation, etoposide, cisplatin (40–42), and reactive oxygen species inducers (43). Moreover, UPR-inducing drugs sensitize glioblastoma cells to the alkylating agent temozolomide (44, 45).

We therefore assessed clonogenic survival following alkylation treatment in *AAG* knockdown shA3 cells and in control T98G cells. *AAG* knockdown cells had significantly decreased survival after treatment with MMS (Fig. 5*A*) or temozolomide (Fig. 5*B*). Importantly, cell survival was significantly reduced in AAG-depleted cells at doses of MMS and temozolomide that only modestly reduced viability in control cells. That decreased AAG levels correlate with increased alkylation sensitivity could be explained by a lower DNA repair capacity (17, 46) but contrast with multiple reports linking increased AAG levels with

enhanced alkylation sensitivity (5). Nevertheless, our results showing that AAG is required for alkylation-induced UPR induction suggests alkylation sensitivity may not solely depend on DNA repair but also on the adaptive response induced by ER stress to promote survival.

To further address the biological relevance of alkylation-induced ER stress in this model, we next treated the glioblastoma cell lines with a nontoxic dose of temozolomide (0.2 μM), either alone or in combination with salinomycin (0.1 μM), an ionophore agent known to induce ER stress and to activate the UPR leading to XBP1 splicing and BiP upregulation (37). Salinomycin treatment sensitizes glioblastoma cells to temozolomide, and survival after temozolomide and salinomycin cotreatment is reduced in AAG-expressing cells (Fig. 5 *C* and *D*). Strikingly, *AAG* knockdown protects cells against salinomycin, alone or in combination with temozolomide, demonstrating that AAG-mediated UPR induction contributes to cytotoxicity in this cell type.

Finally, we probed the requirements for XBP1 by assessing whether silencing XBP1 in *AAG* knockdown and control cells affects viability to MMS (*SI Appendix*, Fig. S11). We show that *XBP1* knockdown increases the resistance of control T98G and shNS cells to MMS, indicating that alkylation-induced XBP1 activation contributes to cytotoxicity in this system. However, MMS sensitivity of an *AAG XBP1* double knockdown was no greater than the MMS sensitivity of the single *AAG* knockdown shA3 cells, suggesting that AAG is required for MMS-induced XBP1 activation that would lead to cell death. The epistasis of the *AAG* knockdown over XBP1 suggests that *AAG* knockdown inactivates XBP1-dependent alkylation response cellular processes.

Taken together, our data are consistent with the conclusion that alkylation, signaling through AAG, induces hallmarks of an ER stress response. Whether this cascade results in cell death is likely to depend on signal strength and timing, cell type, and physiological context (34).

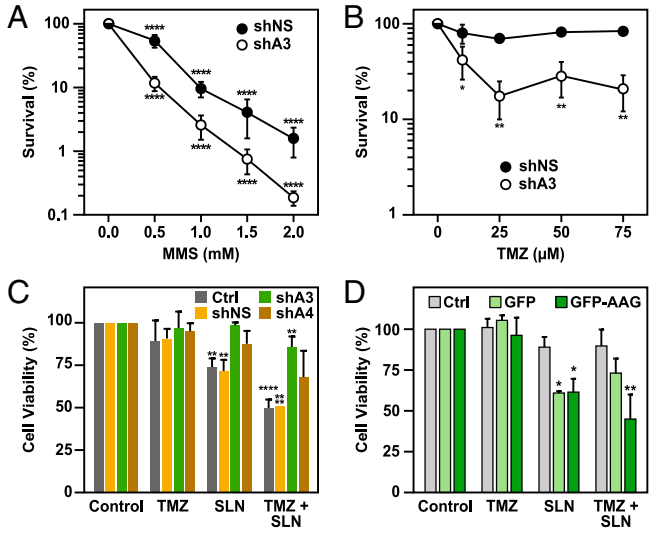

Fig. 5. AAG-mediated UPR induction plays a role in survival to alkylation. (*A* and *B*) Clonogenic survival for cells treated with MMS (0.5 to 2 mM) for 1 h or temozolomide (TMZ; 10 to 75 μM) for 5 d and incubated in drug-free media for up to 14 d. shA3 cells were more sensitive than shNS cells to MMS (*A*) or TMZ (*B*). (*C* and *D*) MTS survival for cells treated with TMZ (0.2 μM) for 5 d singly or in combination with salinomycin (SLN; 0.1 μM). (*C*) MTS survival for shA3 and shA4 cells compared to wild-type T98G (Ctrl) and shNS cells. (*D*) MTS survival for cells overexpressing AAG (GFP-AAG) compared to cells with low endogenous AAG expression (Ctrl or GFP). The results are expressed as mean values ± SEM from three independent experiments and are represented as cell viability relative to nontreated cells (= 100%) $*P < 0.05$ $**P < 0.01$, $****P < 0.0001$.

Discussion

Cancer chemotherapy relies on DNA damage induction by reactive compounds that are often also proteotoxic, thus increasing focus has been placed on the potential intersection between the UPR and genome damage response pathways. The present work uncovers a role for AAG, a DNA repair enzyme, in the activation of the UPR in response to alkylating chemotherapeutic agents. We show here that alkylation treatment activates the UPR both in mouse liver and glioblastoma cells. We find that AAG modulates alkylation-induced UPR in a mechanism involving XBP1 splicing. Crucially, our results suggest this modulation does not depend on the DNA repair activity of AAG.

Alkylating agents target a variety of cellular macromolecules, including proteins. Although our study in the mouse liver examines alkylation-induced transcriptional reprogramming in repair-deficient mice, they are mirrored by studies in *Saccharomyces cerevisiae* that similarly showed transcriptional induction of the UPR by alkylation treatment (19, 38). Finally, UPR induction was shown to be important for alkylation survival in *Drosophila*, murine, and human cell models (21, 27). Our work now shows that alkylation induces the UPR through a pathway that involves AAG and XBP1.

Upregulation of UPR markers has been detected in glioblastoma and other cancer types, with implications for cancer progression and response to therapy. The IRE1α/XBP1 branch of the UPR has been implicated in glioblastoma prognosis (47), potentially by promoting glioma infiltration and motility through the modulation of proangiogenic and proinflammatory chemokines (48, 49). While our results support a role for the IRE1α/XBP1 branch in alkylation-induced UPR, we cannot rule out the participation of other UPR branches, namely, PERK and ATF6. ATF6 reportedly affects glioblastoma development and radiotherapy resistance (40), while PERK is important for glioblastoma growth and survival (41). Given the importance of the UPR in cancer, a better understanding of how AAG affects alkylation-induced UPR could advance efforts for therapeutically targeting ER stress/UPR in cancer.

Our gene expression analyses in the MMS-treated mouse liver show that the transcriptional response to alkylation treatment is profoundly reduced in the absence of Aag. Besides the enrichment for ER stress/UPR-related transcripts and the overlap with multiple gene sets induced by ER stress-inducing drugs (*SI Appendix*, Fig. S2), we find that genes induced by MMS in wild-type liver also significantly overlap with single gene perturbations associated with specific biological phenotypes related to ER redox homeostasis (overexpression of *ERO1L*), UPR (*H6pd* knockout), and recovery from inflammation and toxicity (*Socs3*, *Mat1a*, and *Txnrd1* knockouts) (Dataset 2). In contrast, Aag-deficient mice do not exhibit alterations in the expression of these markers of tissue injury. This is consistent with previous work showing that *Aag* knockout protects from alkylation-induced cell death (16), and with a role for Aag in promoting alkylation-induced tissue injury.

AAG-mediated alkylation-induced toxicity is rescued in animals that lack Parp-1 (16). It is thought that AAG-initiated BER followed by DNA strand cleavage induces PARP-1 activation that results in tissue damage by depleting cells of energy, which leads to necrosis. It is not clear whether AAG-mediated UPR is an additional pathway of cell death induction that contributes to alkylation-induced tissue damage. Nevertheless, our results suggest PARP-1 activation is not necessary for AAG-mediated UPR, at least as it relates to XBP1 splicing. It is worthy of mention that PARP-1 has been previously shown to promote enhanced activity of the 20S proteasome in response to oxidative damage, thus contributing to the removal of oxidized nuclear proteins (50, 51). Our results do not exclude the

possibility that PARP-1 could play a similar BER-independent role in response to alkylated proteins.

Our data indicate that a mutant AAG variant defective in base excision nevertheless complements some alkylation-responsive phenotypes as measured in AAG-deficient cells, namely, γH2AX foci formation and XBP1 splicing. This indicates that alkylation-induced γH2AX foci formation may occur, at least in part, independently of AAG base excision activity, and that the connection between the UPR and AAG can proceed in the absence of BER initiation and PARP-1 activation. This is an important consideration because increased AAG levels have been associated with increased inflammation and increased genetic instability in the form of increased microsatellite instability (MSI) (52). Moreover, overexpression of the corresponding human AAG-Y127I/H136L double mutant led to increased MSI in cultured human K562 cells (36). Our results showing that a catalytically inactive AAG protein can still induce γH2AX and the DDR suggest that some of the effects of AAG may derive from its ability to recognize damaged bases. Recently, a catalytically inactive mutant of 8-oxoguanine DNA glycosylase (OGG1) was shown to act as a potent regulator of gene expression, and substrate binding was required for OGG1-driven transcriptional activation (53). Similarly, AAG-mediated recognition of alkylated bases could initiate signaling that propagates toward XBP1 splicing. One potential scenario would be a catalytically inactive AAG mutant retaining the ability to bind the abundant alkylation-induced N7-guanine adducts, which are neither mutagenic nor toxic but could represent a block to replication and/or transcription if bound by the catalytically dead AAG. Alternatively, AAG may have a role in alkylation-induced UPR that is independent of DNA binding. Our results indicate that AAG affects cellular responses to alkylation by playing independent roles in BER and UPR induction; AAG's role in BER depends on its glycosylase activity and leads to PARP activation, while the UPR role is independent of its glycosylase activity and works via XBP1. Whether substrate binding is required for the activation of the AAG-XBP1 axis and UPR, however, still remains to be determined.

The biochemical properties of the AAG protein of binding to and excising damaged bases have important implications for the dynamics of DNA transactions (e.g., repair, replication, and transcription) in the presence of physiological or supraphysiological levels of DNA damage. Our results support a model where AAG exerts its effects through binding damaged DNA and interacting with other proteins associated with DNA transactions. It has been reported that wild-type AAG interacts with a number of other proteins with known roles in transcriptional modulation and/or ubiquitin-mediated proteolytic pathways, including HR23A, HR23B, p53, and estrogen receptor alpha (54–56). More recently, AAG was shown to form a complex with active RNA pol II through direct binding to the ELP1 subunit of the transcriptional elongator complex (57). The interaction between AAG and ELP1 could be important for a robust transcriptional response in alkylation-induced UPR, given that ELP1 deficiency was shown to disrupt protein homeostasis and induce the UPR (58). AAG is also reported to interact with MBD1, a methyl-CpG binding domain protein implicated in transcriptional regulation (59), and ubiquitin-like with PHD and RING Finger domains 1 and 2 (UHRF1/2) proteins, "hub" proteins involved in epigenetic regulation (60). Therefore, AAG could affect the UPR through its interaction with proteins important for ER stress response or transcriptional control in general.

DNA repair and the UPR were previously reported to cooperate in response to cellular stress. In particular, an important subset of XBP1 targets are DNA repair genes (61). ER stress induction was reported to modulate the expression of BER proteins, including AAG (62, 63) and APEX1 (64). Furthermore, pharmacological ER stress induction potentiated the cytotoxic effects of temozolomide in glioblastoma cells (62, 63). These results implicate ER stress/UPR in DNA repair modulation and indicate that the two pathways cooperate in stress response.

Together, our results demonstrate the DNA repair enzyme AAG plays a role in alkylation-induced UPR activation. Whether there is a direct effect of AAG on alkylation-induced UPR or whether it is due to AAG-mediated DNA damage recognition remains to be defined, but our data strongly suggest that AAG's base excision activity is not required. We anticipate that a detailed mechanistic dissection of this stress response crosstalk will lead to a better understanding of cellular outcomes upon alkylation exposure and may shape future advances in the prevention and treatment of cancer and other age-related diseases.

Materials and Methods

Materials. MMS, puromycin, salinomycin, temozolomide, and Dulbecco's modified Eagle's medium low glucose were from Sigma. Cell culture reagents were from Invitrogen.

Mice. *Aag* null mice were described previously (24). Details about animal experiments are described in the *SI Appendix*. The Massachusetts Institute of Technology (MIT) Committee for Animal Care approved all animal procedures.

Microarray Processing and Data Analysis. Messenger RNA was isolated, amplified, and hybridized onto Affymetrix GeneChip Mouse Genome 430A 2.0 arrays according to the protocols suggested by Affymetrix. Data were analyzed using R/Bioconductor as described in the *SI Appendix*. R scripts are available at https://github.com/nohturfft/Milano_et_al_2022.

Plasmids. Plasmid pEGFP-hAAG was generated by cloning the XhoI-flanked *AAG* cDNA from pCAGGS-hAAG (36), into pEGFP-C3 or into pEGFP-N1 (Clontech, Takara BioUSA, Inc). Plasmid pCAGGS with the mAag-Y147I/H156L double mutant cDNA was generated by site-directed mutagenesis of the wild-type cDNA, as previously described (36). Knockdown resistant wild-type and Y127I/H136L double mutant human AAG cDNAs were generated by site-directed mutagenesis, using the Q5 Site-Directed Mutagenesis kit (E0554S; New England BioLabs). Primers used to mutagenize the human AAG cDNA are listed in *SI Appendix*, Table S1. The nucleotide sequence of all plasmids was confirmed by DNA sequencing. Lentiviral shRNA plasmids based on pGIPZ were purchased from Dharmacon; insert sequences are listed in *SI Appendix*, Table S2.

Cell Culture. A172 and T98G human glioblastoma cell lines were obtained from ATCC, were free from mycoplasma contamination, and were always used from a young stock. Experimental details related to cell culture and cell line development and complementation are described in the *SI Appendix*.

AAG Activity Assay. AAG activity assay is described in the *SI Appendix*.

XBP1 Splicing and Expression Analysis. Quantitative and qualitative PCR methods and reagents are described in the *SI Appendix* .

Immunoblotting and PAR and γH2AX Detection. For details on immunoblotting and antibodies, see *SI Appendix*.

Statistical Analysis. Unless otherwise stated, results are presented as mean ± SEM, and analyses are results of three or more independent experiments. Statistical calculations were performed with GraphPad Prism software, version 6.0.

Data Availability. Microarray data have been deposited in the Gene Expression Omnibus (GSE115254). All study data are included in the article and/or supporting information.

ACKNOWLEDGMENTS. We thank Rebecca Fry, Katherine Pease, Jennifer Calvo, Fugen Li, and Stuart Levine (MIT BioMicroCenter) for help with the gene expression analysis and Joanna Klapacz for the plasmid containing the double-mutant mouse Aag variant. We thank Miriana Machado (Federal University of Rio Grande do Sul, Brazil) for clerical support. The National Institutes of Environmental Health Sciences (ES11399) funded work performed at MIT. Work was otherwise supported by a grant from the Royal Society (RC3532) and the Conselho Nacional de Desenvolvimento Científico e Tecnológico (CNPq; awards 400557/2013-4 and 207503/2015-0). L.M., C.F.C., and R.A. are recipients of Science without Borders studentships (CNPq). L.B.M. was supported by an international visiting professorship grant (CNPq). The authors declare no conflict of interest.

1. A. Vihervaara, F. M. Duarte, J. T. Lis, Molecular mechanisms driving transcriptional stress responses. *Nat. Rev. Genet.* **19**, 385–397 (2018).
2. S. Maynard, E. F. Fang, M. Scheibye-Knudsen, D. L. Croteau, V. A. Bohr, DNA damage, DNA repair, aging, and neurodegeneration. *Cold Spring Harb. Perspect. Med.* **5**, a025130 (2015).
3. N. Dicks, K. Gutierrez, M. Michalak, V. Bordignon, L. B. Agellon, Endoplasmic reticulum stress, genome damage, and cancer. *Front. Oncol.* **5**, 11 (2015).
4. F. Drabløs *et al.*, Alkylation damage in DNA and RNA—Repair mechanisms and medical significance. *DNA Repair (Amst.)* **3**, 1389–1407 (2004).
5. D. Fu, J. A. Calvo, L. D. Samson, Balancing repair and tolerance of DNA damage caused by alkylating agents. *Nat. Rev. Cancer* **12**, 104–120 (2012).
6. C. Y. Liu *et al.*, Kaohsiung Leukemia Research Group, Cured meat, vegetables, and bean-curd foods in relation to childhood acute leukemia risk: A population based case-control study. *BMC Cancer* **9**, 15 (2009).
7. M. Hidajat *et al.*, Lifetime cumulative exposure to rubber dust, fumes and N-nitrosamines and non-cancer mortality: A 49-year follow-up of UK rubber factory workers. *Occup. Environ. Med.* **76**, 250–258 (2019).
8. C. M. White, Understanding and preventing (*N*-nitrosodimethylamine) NDMA contamination of medications. *Ann. Pharmacother.* **54**, 611–614 (2020).
9. M. Tong *et al.*, Nitrosamine exposure causes insulin resistance diseases: Relevance to type 2 diabetes mellitus, non-alcoholic steatohepatitis, and Alzheimer's disease. *J. Alzheimers Dis.* **17**, 827–844 (2009).
10. S. M. de la Monte, M. Tong, Mechanisms of nitrosamine-mediated neurodegeneration: Potential relevance to sporadic Alzheimer's disease. *J. Alzheimers Dis.* **17**, 817–825 (2009).
11. G. L. Dianov, U. Hübscher, Mammalian base excision repair: The forgotten archangel. *Nucleic Acids Res.* **41**, 3483–3490 (2013).
12. F. A. Alhumaydhi *et al.*, Alkyladenine DNA glycosylase deficiency uncouples alkylation-induced strand break generation from PARP-1 activation and glycolysis inhibition. *Sci. Rep.* **10**, 2209 (2020).
13. M. Ensminger *et al.*, DNA breaks and chromosomal aberrations arise when replication meets base excision repair. *J. Cell Biol.* **206**, 29–43 (2014).
14. L. B. Meira *et al.*, Aag-initiated base excision repair drives alkylation-induced retinal degeneration in mice. *Proc. Natl. Acad. Sci. U.S.A.* **106**, 888–893 (2009).
15. M. Allocca, J. J. Corrigan, K. R. Fake, J. A. Calvo, L. D. Samson, PARP inhibitors protect against sex- and AAG-dependent alkylation-induced neural degeneration. *Oncotarget* **8**, 68707–68720 (2017).
16. J. A. Calvo *et al.*, Aag DNA glycosylase promotes alkylation-induced tissue damage mediated by Parp1. *PLoS Genet.* **9**, e1003413 (2013).
17. S. Agnihotri *et al.*, Alkylpurine-DNA-N-glycosylase confers resistance to temozolomide in xenograft models of glioblastoma multiforme and is associated with poor survival in patients. *J. Clin. Invest.* **122**, 253–266 (2012).
18. S. Fosmark *et al.*, APNG as a prognostic marker in patients with glioblastoma. *PLoS One* **12**, e0178693 (2017).
19. S. A. Jelinsky, L. D. Samson, Global response of *Saccharomyces cerevisiae* to an alkylating agent. *Proc. Natl. Acad. Sci. U.S.A.* **96**, 1486–1491 (1999).
20. X. Z. Wang *et al.*, Signals from the stressed endoplasmic reticulum induce C/EBP-homologous protein (CHOP/GADD153). *Mol. Cell. Biol.* **16**, 4273–4280 (1996).
21. A. Zanotto-Filho *et al.*, Combined gene expression and RNAi screening to identify alkylation damage survival pathways from fly to human. *PLoS One* **11**, e0153970 (2016).
22. C. Hetz, F. R. Papa, The unfolded protein response and cell fate control. *Mol. Cell* **69**, 169–181 (2018).
23. H. Urra, E. Dufey, T. Avril, E. Chevet, C. Hetz, Endoplasmic reticulum stress and the hallmarks of cancer. *Trends Cancer* **2**, 252–262 (2016).
24. B. P. Engelward *et al.*, Base excision repair deficient mice lacking the Aag alkyladenine DNA glycosylase. *Proc. Natl. Acad. Sci. U.S.A.* **94**, 13087–13092 (1997).
25. M. V. Kuleshov *et al.*, Enrichr: A comprehensive gene set enrichment analysis web server 2016 update. *Nucleic Acids Res.* **44** (W1), W90–W97 (2016).
26. E. Y. Chen *et al.*, Enrichr: Interactive and collaborative HTML5 gene list enrichment analysis tool. *BMC Bioinformatics* **14**, 128 (2013).
27. A. Zanotto-Filho *et al.*, Alkylating agent-induced NRF2 blocks endoplasmic reticulum stress-mediated apoptosis via control of glutathione pools and protein thiol homeostasis. *Mol. Cancer Ther.* **15**, 3000–3014 (2016).
28. M. F. Gregor *et al.*, The role of adipocyte XBP1 in metabolic regulation during lactation. *Cell Rep.* **3**, 1430–1439 (2013).
29. J. Argemí *et al.*, X-box binding protein 1 regulates unfolded protein, acute-phase, and DNA damage responses during regeneration of mouse liver. *Gastroenterology* **152**, 1203–1216 (2017).
30. L. M. Brignull *et al.*, Reprogramming of lysosomal gene expression by interleukin-4 and Stat6. *BMC Genomics* **14**, 853 (2013).
31. B. P. Gomez *et al.*, Human X-box binding protein-1 confers both estrogen independence and antiestrogen resistance in breast cancer cell lines. *FASEB J.* **21**, 4013–4027 (2007).
32. H. Yoshida, T. Matsui, A. Yamamoto, T. Okada, K. Mori, XBP1 mRNA is induced by ATF6 and spliced by IRE1 in response to ER stress to produce a highly active transcription factor. *Cell* **107**, 881–891 (2001).
33. M. Weller *et al.*, European Association for Neuro-Oncology (EANO) Task Force on Malignant Glioma, EANO guideline for the diagnosis and treatment of anaplastic gliomas and glioblastoma. *Lancet Oncol.* **15**, e395–e403 (2014).
34. S. J. M. Healy, A. M. Gorman, P. Mousavi-Shafaei, S. Gupta, A. Samali, Targeting the endoplasmic reticulum-stress response as an anticancer strategy. *Eur. J. Pharmacol.* **625**, 234–246 (2009).
35. M. Bi *et al.*, ER stress-regulated translation increases tolerance to extreme hypoxia and promotes tumor growth. *EMBO J.* **24**, 3470–3481 (2005).
36. J. Klapacz *et al.*, Frameshift mutagenesis and microsatellite instability induced by human alkyladenine DNA glycosylase. *Mol. Cell* **37**, 843–853 (2010).
37. T. Li *et al.*, Salinomycin induces cell death with autophagy through activation of endoplasmic reticulum stress in human cancer cells. *Autophagy* **9**, 1057–1068 (2013).
38. S. A. Jelinsky, P. Estep, G. M. Church, L. D. Samson, Regulatory networks revealed by transcriptional profiling of damaged *Saccharomyces cerevisiae* cells: Rpn4 links base excision repair with proteasomes. *Mol. Cell. Biol.* **20**, 8157–8167 (2000).
39. M. C. Caron *et al.*, Poly(ADP-ribose) polymerase-1 antagonizes DNA resection at double-strand breaks. *Nat. Commun.* **10**, 2954 (2019).
40. D. Y. A. Dadey *et al.*, The ATF6 pathway of the ER stress response contributes to enhanced viability in glioblastoma. *Oncotarget* **7**, 2080–2092 (2016).
41. X. Hou *et al.*, PERK silence inhibits glioma cell growth under low glucose stress by blockage of p-AKT and subsequent HK2's mitochondria translocation. *Sci. Rep.* **5**, 9065 (2015).
42. H. K. Lee *et al.*, GRP78 is overexpressed in glioblastomas and regulates glioma cell growth and apoptosis. *Neuro-oncol.* **10**, 236–243 (2008).
43. Y. Liu *et al.*, Targeting X box-binding protein-1 (XBP1) enhances sensitivity of glioma cells to oxidative stress. *Neuropathol. Appl. Neurobiol.* **37**, 395–405 (2011).
44. L. M. Epple *et al.*, Induction of the unfolded protein response drives enhanced metabolism and chemoresistance in glioma cells. *PLoS One* **8**, e73267 (2013).
45. P. Pyrko, A. H. Schönthal, F. M. Hofman, T. C. Chen, A. S. Lee, The unfolded protein response regulator GRP78/BiP as a novel target for increasing chemosensitivity in malignant gliomas. *Cancer Res.* **67**, 9809–9816 (2007).
46. D. Svilar *et al.*, Alkylation sensitivity screens reveal a conserved cross-species functionome. *Mol. Cancer Res.* **10**, 1580–1596 (2012).
47. O. Pluquet *et al.*, Posttranscriptional regulation of PER1 underlies the oncogenic function of IREα. *Cancer Res.* **73**, 4732–4743 (2013).
48. A. Jabouille *et al.*, Glioblastoma invasion and cooption depend on IRE1α endoribonuclease activity. *Oncotarget* **6**, 24922–24934 (2015).
49. G. Auf *et al.*, Inositol-requiring enzyme 1alpha is a key regulator of angiogenesis and invasion in malignant glioma. *Proc. Natl. Acad. Sci. U.S.A.* **107**, 15553–15558 (2010).
50. O. Ullrich *et al.*, Poly-ADP ribose polymerase activates nuclear proteasome to degrade oxidatively damaged histones. *Proc. Natl. Acad. Sci. U.S.A.* **96**, 6223–6228 (1999).
51. B. Catalgol *et al.*, Chromatin repair after oxidative stress: Role of PARP-mediated proteasome activation. *Free Radic. Biol. Med.* **48**, 673–680 (2010).
52. L. J. Hofseth *et al.*, The adaptive imbalance in base excision-repair enzymes generates microsatellite instability in chronic inflammation. *J. Clin. Invest.* **112**, 1887–1894 (2003).
53. W. Hao *et al.*, Enzymatically inactive OGG1 binds to DNA and steers base excision repair toward gene transcription. *FASEB J.* **34**, 7427–7441 (2020).
54. F. Miao *et al.*, 3-Methyladenine-DNA glycosylase (MPG protein) interacts with human RAD23 proteins. *J. Biol. Chem.* **275**, 28433–28438 (2000).
55. S. Song *et al.*, N-methylpurine DNA glycosylase inhibits p53-mediated cell cycle arrest and coordinates with p53 to determine sensitivity to alkylating agents. *Cell Res.* **22**, 1285–1303 (2012).
56. V. S. Likhite, E. I. Cass, S. D. Anderson, J. R. Yates, A. M. Nardulli, Interaction of estrogen receptor alpha with 3-methyladenine DNA glycosylase modulates transcription and DNA repair. *J. Biol. Chem.* **279**, 16875–16882 (2004).
57. N. P. Montaldo *et al.*, Alkyladenine DNA glycosylase associates with transcription elongation to coordinate DNA repair with gene expression. *Nat. Commun.* **10**, 5460 (2019).
58. J. Goffena *et al.*, Elongator and codon bias regulate protein levels in mammalian peripheral neurons. *Nat. Commun.* **9**, 889 (2018).
59. S. Watanabe *et al.*, Methylated DNA-binding domain 1 and methylpurine-DNA glycosylase link transcriptional repression and DNA repair in chromatin. *Proc. Natl. Acad. Sci. U.S.A.* **100**, 12859–12864 (2003).
60. C. Liang *et al.*, Identification of UHRF1/2 as new N-methylpurine DNA glycosylase-interacting proteins. *Biochem. Biophys. Res. Commun.* **433**, 415–419 (2013).
61. D. Acosta-Alvear *et al.*, XBP1 controls diverse cell type- and condition-specific transcriptional regulatory networks. *Mol. Cell* **27**, 53–66 (2007).
62. E. Xipell *et al.*, Endoplasmic reticulum stress-inducing drugs sensitize glioma cells to temozolomide through downregulation of MGMT, MPG, and Rad51. *Neuro-oncol.* **18**, 1109–1119 (2016).
63. J. L. Weatherbee, J. L. Kraus, A. H. Ross, ER stress in temozolomide-treated glioblastomas interferes with DNA repair and induces apoptosis. *Oncotarget* **7**, 43820–43834 (2016).
64. T. L. Cheng *et al.*, Induction of apurinic endonuclease 1 overexpression by endoplasmic reticulum stress in hepatoma cells. *Int. J. Mol. Sci.* **15**, 12442–12457 (2014).